ACS OMEGA

http://pubs.acs.org/journal/acsodf

Article

Gold–Silver Bimetallic Nanoparticles Reduced with Herbal Leaf Extracts Induce ROS-Mediated Death in Both Promastigote and Amastigote Stages of *Leishmania donovani*

Dayakar Alti, M. Veeramohan Rao, D. Narayana Rao, Radheshyam Maurya,* and Suresh K. Kalangi*

Cite This: *ACS Omega* 2020, 5, 16238–16245

Read Online

ACCESS | Metrics & More | Article Recommendations | Supporting Information

ABSTRACT: Resistance to antileishmanial drugs such as sodium stibogluconate (SSG), amphotericin B (Amp-B), and miltefosine is on the rise, and alternate strategies for effective treatment have gained importance in recent years. Although nanoparticle (NP)-based composite drugs that have emerged recently have been found to be effective, the associated toxicity limits their usage. Bimetallic NPs produced through reduction with medicinal plant extracts are proposed to overcome the toxicity of the NPs. In the present study, three types of gold–silver bimetallic nanoparticles (Au–Ag BNPs) were synthesized through a single-step reduction process using fenugreek, coriander, and soybean leaf extracts. All of the three types of BNPs exhibited high antileishmanial effects against promastigotes with half-inhibitory concentration (IC_{50}) values in the range of 0.03–0.035 μg/mL. The IC_{50} values of the BNPs are much lower compared to those of miltefosine (IC_{50} = 10 μg/mL). The synthesized BNPs induced the reactive oxygen species (ROS)-mediated apoptosis-like death in the promastigotes and could potentiate the antileishmanial activity of macrophages. The intracellular amastigotes were reduced by 31–46% in macrophages. The biogenic BNPs synthesized in this study and their potent antileishmanial activity provide further impetus to the ongoing quest for novel drugs to effectively manage leishmaniasis.

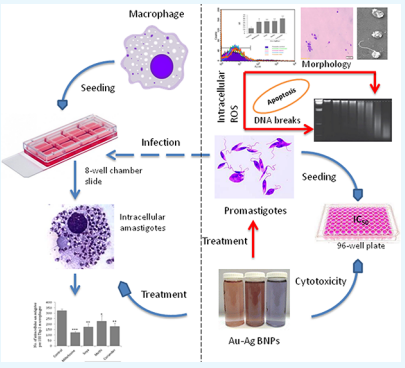

INTRODUCTION

Leishmaniasis is a tropical disease caused by the intracellular parasite *Leishmania* and is transmitted by female *Phlebotomine* sand flies. The disease is highly prevalent among the poor population of the world, living in tropical and subtropical countries. Infected individuals are observed to develop problems ranging from self-healing cutaneous lesions to life-threatening visceral disease.[1−4] Worldwide, about 0.7−1.0 million new cases and 20 000−30 000 deaths due to leishmaniasis are reported annually.[2] Among the clinical forms, visceral leishmaniasis (VL) or kala-azar is the most fatal, which is typically caused by *Leishmania donovani* in the Indian subcontinent. Every year, about 50 000−90 000 new VL cases are reported around the globe, with a high incidence in the Indian subcontinent and East Africa.[2] VL is emerging as an opportunistic coinfection and is posing a threat in acquired immunodeficiency syndrome (AIDS) patients.[3] The clinical symptoms of VL include fever, weight loss, anemia, pancytopenia, hyperpigmentation of skin, and hepatosplenomegaly, and the mortality rate is relatively higher (about 95%) in VL patients.[2] Treatment mostly relies on chemotherapy, which is limited to a few drugs including pentavalent antimonials (Sb^V), amphotercin B (Amp-B), miltefosine, and paromomycin. High costs, life-threatening toxicity, and, more importantly, development of clinical resistance have been an impediment in using these drugs.[5] Increased activity of membrane-associated efflux pumps on parasites, low bioavailability of drugs, reduced exposure time of drugs, delayed conversion rate of the prodrug forms to get activated,[6] and plasticity of the parasite genome[7] have been identified as predominant reasons to drug resistance in Leishmaniasis treatment. Further resistance has also been reported for miltefosine/paromomycin and sodium stibogluconate (SSG)/paromomycin combination therapies.[8] In the light of increasing drug resistance against existing drugs, nanoparticle (NP)-based drugs have become one of the best options to combat resistance, and they have become the focus in search of developing alternate strategies for effective treatment of leishmaniasis.

In the recent past, although chemically synthesized NPs have been proposed for effective treatment of leishmaniasis,[9−12] their toxicity on macrophages has limited their applications. However, NPs synthesized by green chemistry have assumed significance as alternatives with their biocompatible nature. Biogenic silver nanoparticles (AgNPs) were found to be more

Received: May 2, 2020
Accepted: June 9, 2020
Published: June 24, 2020

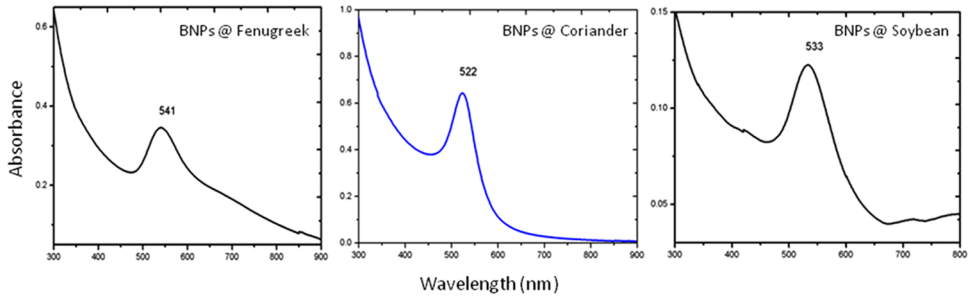

Figure 1. UV−visible spectra of Au−Ag BNPs for fenugreek, coriander, and soybean; the *X*-axis represents wavelength (nm), and the *Y*-axis represents the absorbance of extracts.

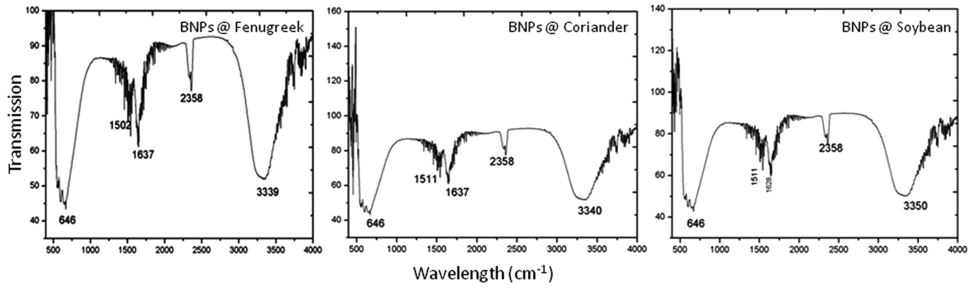

Figure 2. FTIR spectra of Au−Ag BNPs for fenugreek, coriander, and soybean; the *X*-axis represents wavelength (cm^{-1}), and the *Y*-axis represents the transmission.

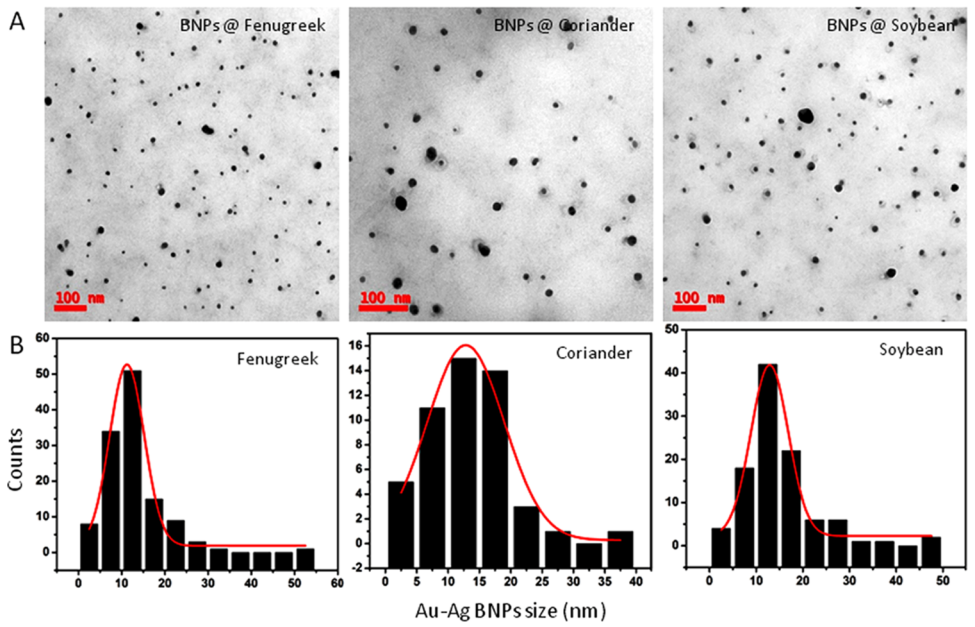

Figure 3. (A) TEM images (scale 100 nm) showing regular and sphere-shaped Au−Ag BNPs for fenugreek, coriander, and soybean. (B) Histograms showing the average size of BNPs as 10−12 nm; the *X*-axis represents the BNP size (nm), and the *Y*-axis represents the count.

efficient than chemically synthesized AgNPs against *Leishmania amazonensis* promastigotes. With lower concentrations than Amp-B, biosynthetic AgNPs showed an equal effect on the inhibition of parasitemia, in vivo.[4,13] With increasing evidence on bimetallic nanoparticles (BNPs), recent studies have shown that BNPs are relatively more effective than NPs generated by a single metal. Gold (Au)/Ag NPs[14−17] alone were found to be less effective when compared to Au−Ag BNPs.[18,19] Core−shell Au−Ag BNPs[20] and nontoxic Au−Ag BNPs reduced by *Gloriosa superba*[21] and *Mentha piperita*[22] leaf extracts were reported to exhibit a strong antibacterial activity. However, very little information is available on the effectiveness of BNPs as antileishmanial agents. The activities of Au−Ag BNPs against *L. donovani*[19] and of Ti−Ag BNPs against *Leishmania tropica* (the causative agent of cutaneous leishmaniasis) and *Leishmania infantum* (the causative agent of VL) have been demonstrated. They induce reactive oxygen species (ROS)-mediated death of the parasites.[23] The known promising antimicrobial potential of Au−Ag BNPs and the lack of similar studies on leishmaniasis inspired us to test the effect of BNPs on leishmaniasis. In the present study, we synthesized Au−Ag BNPs by green chemistry by utilizing fenugreek, soybean, and

https://dx.doi.org/10.1021/acsomega.0c02032
ACS Omega 2020, 5, 16238−16245

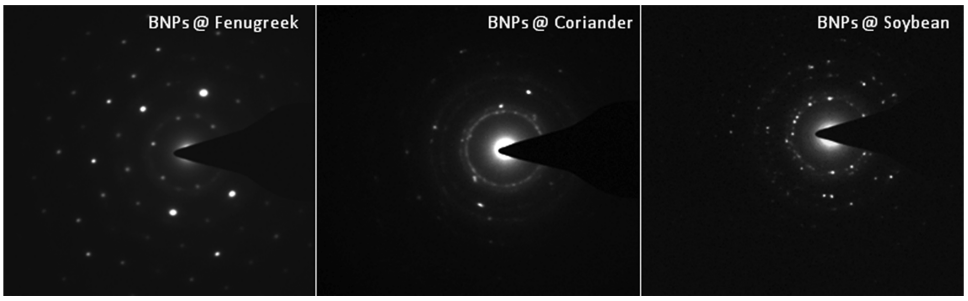

Figure 4. Selected area electron diffraction pattern of Au−Ag BNPs for fenugreek, coriander, and soybean.

coriander leaf extracts separately and tested their activities against *L. donovani* promastigotes and intracellular amastigotes that reside in macrophages.

RESULTS

Ultraviolet (UV)−Visible Absorption Shows Characteristics of Au−Ag BNPs. UV−visible absorption spectral analysis showed peaks at wavelengths of 541, 533, and 522 nm for reduced Au−Ag BNPs generated by fenugreek, soybean, and coriander leaf extracts, respectively (Figure 1). The spectra indicate that the Au−Ag BNPs are in the form of an alloy and not a mixture of individual metal particles. This was further confirmed through lattice constants 0.408 and 0.409 nm for gold and silver, respectively.

Fourier Transform Infrared Spectroscopy (FTIR) Analysis. Au−Ag BNPs made of three leaf extracts of fenugreek, soybean, and coriander exhibited five significant peaks, viz. 646, 1511, 1636, 2358, and 3348 cm^{-1} for all (Figure 2). The peak at 646 cm^{-1} is due to the −CH− out-of-plane bending vibrations being substituted by ethylene systems −CH═CH− (cis). The band center at 1511 cm^{-1} can be attributed to amino acids containing $-NH_2-$ groups. The peak center at 1636 cm^{-1} can be attributed to the C═O stretch of amides of proteins or peptides formed as capping agents derived from all three leaf extracts. The band around 2358 cm^{-1} is due to Au−Ag bimetallic linking to the −CN−, indicating the presence of BNPs in the sample. Finally, the strong peak at 3348 cm^{-1} is due to the presence of the amine group.

Transmission Electron Microscopy (TEM) and Energy-Dispersive X-ray Spectroscopy (EDX) Analyses. The Au−Ag BNPs generated are well separated and appear spherical in shape (Figure 3A). The average particle size ranged from 10 to 12 nm for BNPs generated by fenugreek, coriander, or soybean leaf extract reduction (Figure 3B). The selected area electron diffraction (SAED) pattern shown in Figure 4 for the Au−Ag BNPs generated by the three different leaf extracts provided further evidence of their crystalline nature.

Induction of Cytotoxicity and Structural Aberrations in Promastigotes by Au−Ag BNPs. The ability of Au−Ag BNPs to induce cytotoxicity in promastigotes was tested with an MTT [3-(4,5-dimethylthiazol-2-yl)−2,5-diphenyl tetrazolium bromide] assay. Concentration-dependent cytotoxicity was observed when incubated for 48 h (Figure 5). The half-inhibitory concentration (IC_{50}) values of Au−Ag BNPs synthesized by reduction with leaf extracts of soybean, fenugreek, and coriander were found to be 0.03, 0.035, and 0.035 μg/mL, respectively, whereas the IC_{50} for miltefosine was 10 μg/mL against promastigotes (Figure 5). Light microscopy images of promastigotes treated with the

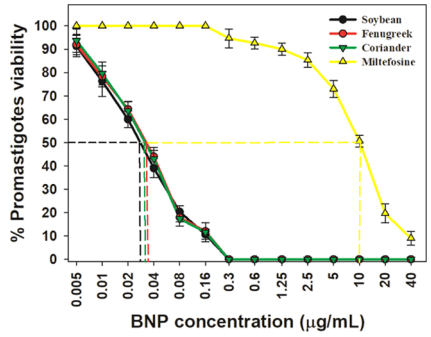

Figure 5. Cytotoxicity of BNPs against *L. donovani* promastigotes; the *X*-axis represents the concentrations of BNPs between 0.005 and 0.16 μg/mL and of miltefosine between 0.3 and 40 μg/mL, and the *Y*-axis represents the percentage viability of promastigotes. IC_{50} of BNPs on promastigotes intercepted with dotted lines.

respective IC_{50} concentration of Au−Ag BNPs for 48 h revealed loss of structural integrity when compared to control parasites (Figure 6A). The untreated promastigotes appeared to have slender bodies and long flagella, whereas BNP-treated promastigotes appeared round/ovoid and majority of them had lost their flagellum. Scanning electron microscopy (SEM) analyses revealed structural abnormalities akin to those observed during apoptosis (Figure 6B).

Induction of DNA Breaks and Intracellular ROS in Promastigotes by Au−Ag BNPs. Genomic DNA fragmentation by endogenous nucleases and the generation of intracellular ROS are the hallmarks of apoptosis in promastigotes.[28] We observed that Au−Ag BNPs induced genomic DNA breaks in promastigotes by 48 h, as it appears like a smear on agarose gel (Figure 6C). To determine the extent of ROS generation by BNPs, the mean fluorescence intensity (MFI) of ROS labeled by the 2′,7′-dichloro dihydrofluorescein (H_2DCF) green fluorescence dye was measured using flow cytometry. The MFI values were 13 ± 4, 32 ± 3, 33 ± 4, and 40 ± 4 for untreated cells and BNPs of soybean, fenugreek, and coriander leaf extracts, respectively (Figure 6D). The MFI was 31 ± 7 in promastigotes treated with miltefosine. These results indicate the induction of apoptosis-like death in promastigotes when treated with BNPs.

Biocompatibility of Au−Ag BNPs with Macrophages. In spite of the wide range of Au−Ag BNP concentrations (0.01−2.5 μg/mL) tested against the human macrophage cell line, we noticed only 20% cell death even at the highest concentration (2.5 μg/mL). The highest concentration of Au−Ag BNPs that we tested against macrophages was ∼70 times higher than that of IC_{50} values (0.03−0.035 μg/mL) that we calculated against promastigotes. If we consider these IC_{50}

https://dx.doi.org/10.1021/acsomega.0c02032
ACS Omega 2020, 5, 16238−16245

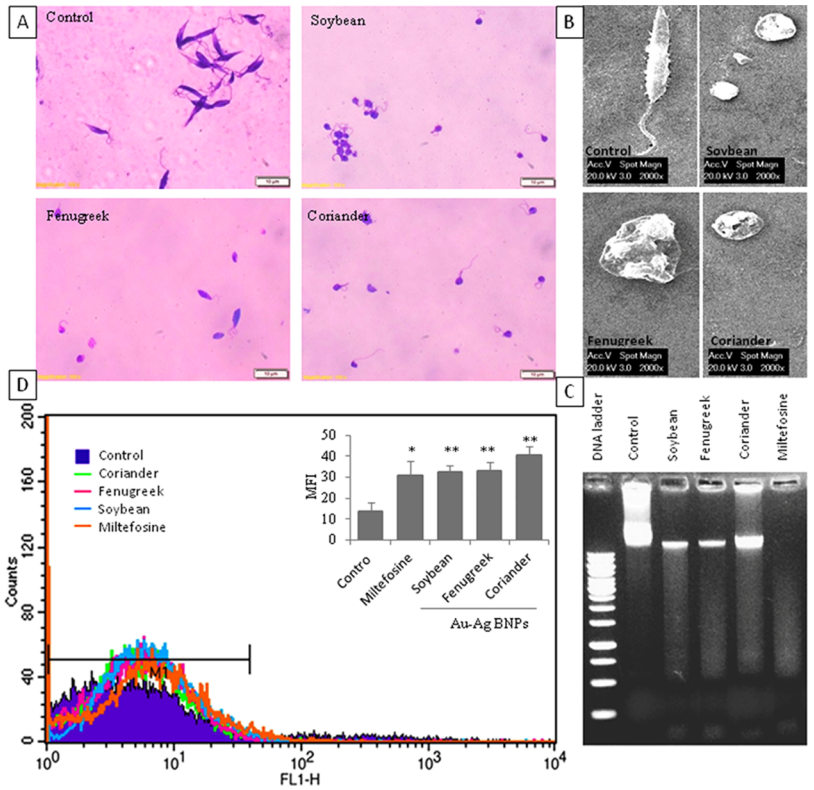

Figure 6. BNPs induced apoptosis-like features in promastigotes. (A) Light microscopy analysis of morphological alteration in Giemsa-stained promastigotes (scale 10 μm). (B) SEM analysis of morphological aberrations in promastigotes (scale 2000×). (C) Genomic DNA fragmentation as a smear in promastigotes. (D) H_2DCF fluorescence intensity measured in the FL1-H channel by a flow cytometer, and intracellular ROS production in promastigotes represented as MFI (insert), "p values" are represented as *$p \leq 0.05$ and **$p \leq 0.01$.

values against macrophages, the percentage death of macrophages was less than 10%. Hence, in the following experiments on macrophages, we used 0.03−0.035 μg/mL concentration of Au−Ag BNPs. As shown in our previous report,[27] here too, miltefosine (1 μg/mL or 2.5 μM) showed ∼80% viability in macrophages (Figure S1).

Depletion of Amastigote Growth Inside Macrophages by Au−Ag BNPs. The ability of BNPs to abrogate amastigote growth inside macrophages was investigated. Localization of amastigotes in the macrophages under different conditions of treatment is shown in Figure 7. The average number of intracellular amastigotes per 100 macrophages was counted; it was 321 ± 19 in untreated macrophages and were 173 ± 30 (i.e., 46% reduction), 224 ± 53 (i.e., 31% reduction), and 178 ± 30 (i.e., 45% reduction) in BNPs of macrophages treated with soybean, fenugreek, and coriander leaf extracts, respectively. The positive drug control miltefosine (1 μg/mL or 2.5 μM) caused 62% reduction (122 ± 10) of amastigote growth (Figure 7).

Induction of ROS-Mediated Death in Amastigotes by Au−Ag BNPs. All three types of BNPs were able to induce ROS inside the macrophages that are infected with amastigotes (Figure 8). The MFI values of BNPs generated by leaf extracts of coriander, fenugreek, and soybean were 284.6 ± 5.7, 275.8 ± 6.9, and 281.9 ± 3.7, respectively, which were higher than that of the infected control (214.3 ± 13.04). On the other hand, *L. donovani*-infected macrophages showed reduced intracellular ROS levels when compared to that of uninfected cells (243.96 ± 9.04), which caused delayed phagolysosome formation[30] and inhibited oxidative killing of the intracellular amastigotes.[31] Miltefosine treatment was used as a positive control for ROS production inside the infected macrophages, and the MFI was 265.5 ± 8.3, which is significantly higher than the infected control.

DISCUSSION

Chemotherapy is still recommended as a gold standard method for the treatment of leishmaniasis.[32] They have several shortcomings, and quite often the treatment is not successful. The potential reasons for failure include low bioavailability and inappropriate localization or low specificity of the drug, drug resistance due to host genetic background,[33] immune deficiency,[34] and malnutrition.[35] Recently, global warming is considered to be spreading leishmaniasis to new geographical regions.[36] After the failure of drug combination therapies,[8] nanotherapy has emerged as a potential alternative to combat drug resistance. It improves drug delivery and bioavailability. The nanoparticulation of antileishmanial drugs such as meglumine antimoniate,[37] antimony sulfide,[38] andrographolide,[39] and curcumin[40] is shown to improve the precise delivery to target cells, which reduced dosage and toxicity to the host cells. However, newer therapies using metal-based nanotherapies emerged to address the problems associated with conventional drugs.

The mono-metal NPs used against *Leishmania* species are required in high concentrations, which cause toxicity to macrophages. For example, AgNPs and AuNPs studied against *L. major* inhibited promastigote proliferation with low concentrations (10−100 μg/mL), but they were equally toxic to macrophages.[9] The AgNPs against *L. tropica* promastigotes were effective at high concentrations (150−200 μg/mL) and toxic to macrophages with >10 μg/mL.[2,41] At these toxic

https://dx.doi.org/10.1021/acsomega.0c02032
ACS Omega 2020, 5, 16238−16245

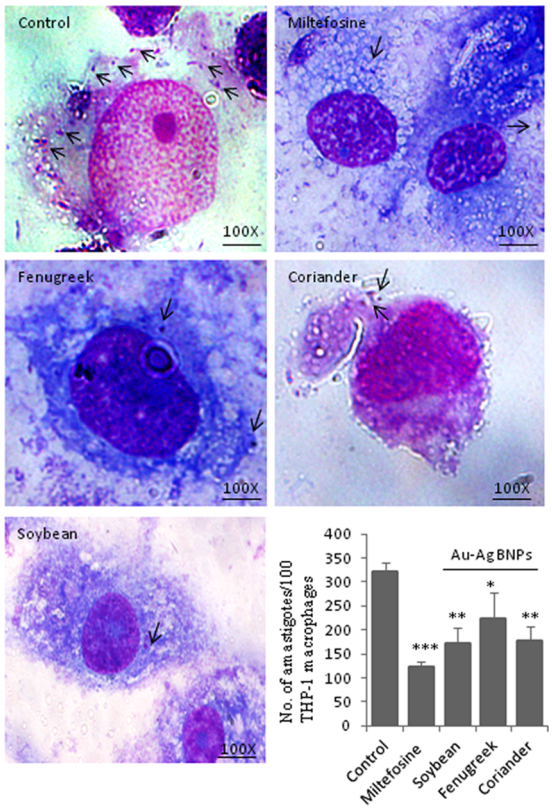

Figure 7. Effect of BNPs on amastigote growth; light microscopic analysis and counting of intracellular amastigotes present inside the Giemsa-stained THP-1 macrophages (scale 100×) and indicated with arrow marks. The average number of amastigotes per 100 macrophages is shown in the bar graph, and p values are represented as $*p \leq 0.05$, $**p \leq 0.01$, and $***p \leq 0.001$.

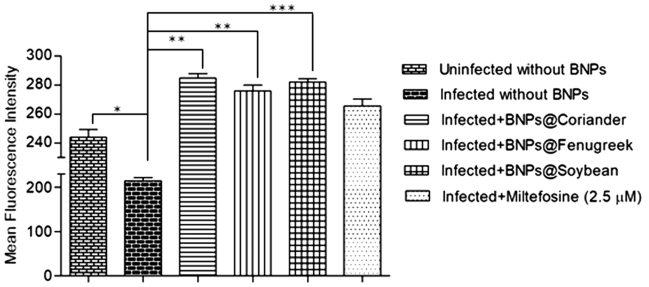

Figure 8. Intracellular ROS production in macrophages. Flow cytometry analysis of ROS levels represented as MFI on the Y-axis of the bar graph. The comparison was done between infected variables with or without BNP treatment. Uninfected cells and infected cells with miltefosine (2.5 μM or 1 μg/mL) treatment are used as controls. The p values are represented as $*p \leq 0.05$, $**p \leq 0.01$, and $***p \leq 0.001$.

concentrations, AgNPs could induce oxidative stress, alterations in the gene expression profile, genetic damage, and necrotic death in higher eukaryotes.[42] In contrast to these, the biogenic mechanisms and the green synthesis method of preparing nanoparticles has several advantages[43] and are biocompatible with the host system. To overcome the limitations associated with mono-metal NPs, the green synthesis of Au−Ag NPs[17,44−46] has been reported as a potential antileishmanial agent. In a comparative study, AgNPs synthesized by chemical and biogenic (*Fusarium oxysporum*) methods reported IC_{50} values of 103.5 ± 11.5 and 31.6 ± 8.2 μM, respectively.[13] Similarly, AgNPs and AuNPs synthesized from *Sargentodoxa cuneata* showed IC_{50} values of about 4.37 and 5.29 μg/mL, respectively, against *L. amazonensis*.[47] These observations highlighted the advantage of phytomaterial composites toward reducing the IC_{50}.

Thus, in this study, we synthesized BNPs using different plant extracts to study the antileishmanial activity. The differential compositions of plant extracts can influence the antileishmanial activity of similar metal NPs. It is evident from the previous[48] report as well as the results of this study that depending on the type of plant extract used, the IC_{50} values varied. The metal salt concentration, reaction time, pH, and temperature can significantly influence the quality, size, and morphology of the synthesized NPs,[49,50] which affect their activity. The monodispersed NPs are more effective than the polydispersed NPs;[51] Au−Ag BNPs in this study are monodispersed with an average size of 10−12 nm, appeared spherical in shape with an organized structure (at 60 min), and showed a remarkable antileishmanial activity.

The spherical shape of BNPs allows them to enter cells[52] via phagocytosis, resulting in the formation of a phagolysosome with an acidified medium (pH 4−5).[53,54] At low pH, Au−Ag BNPs undergo oxidation and release free Au^+ and Ag^+ ions, which target intracellular amastigotes to death. As demonstrated previously with AgNPs, after their phagocytosis by macrophages increases the release of Ag^+ ions by oxidation and favors the death of *L. amazonensis*.[55] In general, macrophages produce high levels of ROS to kill pathogens like viruses, fungi, and parasites.[56] However, the *Leishmania* parasite evades ROS production by macrophages via modulating a few signaling cascade moieties to survive inside phagolysosomes.[57] The intracellular ROS produced by macrophages drives the oxidation of NPs, which further enhances ROS production. We showed that Au−Ag BNPs could activate the macrophages for ROS production and that inhibited amastigote growth to a considerable extent without inducing death in the macrophage population. Results obtained in our study are in agreement with the previously reported mechanism of the action of metal-based NPs. Furthermore, we hypothesize that, along with the ROS, phytochemicals (capping agents) released from BNPs may have good differential effects in infected and uninfected macrophages, which might have boosted the antileishmanial activity through their immune modulatory effects by safeguarding the host cells. However, this is yet to be addressed while studying all possible deeper insight mechanisms of the BNP mechanism of action on the Leishmania parasite.

The three types of BNPs are similarly effective against *L. donovani* promastigotes in causing apoptosis-like death. The IC_{50} values of the BNPs produced against promastigotes are fascinatingly lower (about 285 times) than miltefosine, and the induction of ROS by BNPs in promastigotes was moderately higher when compared to miltefosine. It suggests that BNPs have a better antileishmanial potential than miltefosine on promastigotes. The IC_{50} of Au−Ag BNPs produced against promastigotes proved to be nontoxic to macrophages, which is in contrast to Ti−Ag NPs, whose lethal doses against *L. tropica* promastigotes were found to be toxic to macrophages and the nontoxic concentrations were inefficient against both promastigotes and amastigotes.[23] This important feature of our BNPs is crucial and highlights the importance of selection of metals and plant material to synthesize BNPs. Altogether, this

https://dx.doi.org/10.1021/acsomega.0c02032
ACS Omega 2020, 5, 16238−16245

suggests that the synthesized BNPs appear to be a good alternative for chemotherapy in the near future. As demonstrated earlier, drugs with IC_{50} < 1 μg/mL and selective index (SI) > 20 are highly safe to macrophages and are the best predictors of antiparasitic activity.[58] BNPs used in our study would fit into this category of drugs with the lowest IC_{50} concentrations against *Leishmania*.

CONCLUSIONS

In conclusion, we report the synthesis of Au−Ag BNPs using herbal extracts that reduced metal toxicity. The IC_{50} values of BNPs generated against promastigotes were very low when compared to the standard drug miltefosine. The ability to reduce amastigote survival, induction of apoptosis, and generation of intracellular ROS with BNPs were significant and also comparable to miltefosine. To the best of our knowledge, this is the first report on the antileishmanial activity of BNPs prepared with the leaf extracts of herbs.

EXPERIMENTAL SECTION

Preparation of Leaf Extracts. Fresh leaves (20 g each) of fenugreek, coriander, and soybean were obtained from the fields and thoroughly rinsed with distilled water. The leaves were chopped into small pieces and then boiled in 50 mL distilled water for 5 min; resulting extracts were filtered and cooled to room temperature (RT) and stored at 4 °C until use.

Synthesis of Au−Ag BNPs. The leaf extracts were used as capping and reducing agents for $AgNO_3$ and $HAuCl_4$ to synthesize Au−Ag BNPs. Briefly, an aliquot of 1.5 mL of each extract (fenugreek, coriander, and soybean) was dissolved separately in 15 mL of 10^{-3} M $HAuCl_4$, H_2O, $AgNO_3$, and $HAuCl_4{\cdot}H_2O$ + $AgNO_3$ for fenugreek and coriander (1:1) and for soybean (50:50). Then, the prepared solution was boiled at 80 °C for 30 min, which resulted in the transformation of the colorless solution to a red color, indicating the formation of Au−Ag BNPs. The synthesized Au−Ag BNPs were spun down at 10 416*g* for 30 min and then washed twice with an excess of distilled water; then, the obtained Au−Ag BNPs were used in further biological experiments.

Characterization of Au−Ag BNPs. The JASCO UV−visible spectrometer was used to measure the absorbance of synthesized BNPs. The structural analysis of BNPs was performed using 200 kV ultrahigh-resolution TEM (JEOL-2010). To measure the size of BNPs, carbon-coated copper grids were used by placing a drop of extract on them, followed by drying under a lamp. To determine the composition of elements present in Au−Ag BNPs, we used an EDX detector attached to SEM (JEOL JSM-5300, Japan). To study the presence of functional groups, we performed FTIR analysis using the JASCO FTIR-5300 model.

Cultivation of the Parasite. The experimental parasite strain Dd8 of *L. donovani* promastigotes was obtained from ATCC (American type culture collection) and cultured in a complete M199 (cM199) medium supplemented with 15% heat-inactivated fetal bovine serum (FBS), 20 mM HEPES (4-(2-hydroxyethyl)-1-piperazineethanesulfonic acid), 4 mM $NaHCO_3$, pH 7.4, 100 U/mL penicillin, and 100 mg/mL streptomycin at 25 °C ± 1.

Cytotoxicity Assay on Promastigotes. Cytotoxicity of Au−Ag BNPs on *L. donovani* promastigotes was studied by the MTT assay. In a 96-well plate, log-phase promastigotes (1×10^6 cells/well) were incubated with different concentrations (0.005, 0.01, 0.02, 004, 0.08, and 0.16 μg/mL) of Au−Ag BNPs for 48 h. Selection of this concentration range is based on a previous study on Au−Ag NPs against active and dormant mycobacteria.[24] After incubation, 20 μL of MTT (5 mg/mL) was added and incubated for 4 h at 5% CO_2 and 37 °C. The developed formazan crystals were carefully spun down and dissolved in 150 μL of dimethyl sulfoxide (DMSO). Optical density (OD) was measured at λ_{540nm} using a microplate reader (Quant Bio-tek Instruments, Inc.). Percentage of the parasite viability and IC_{50} values of Au−Ag BNPs were calculated for further use. Miltefosine (concentrations of 0.3, 0.6, 1.25, 2.5, 5, 10, 20, and 40 μg/mL) was the positive control. The experiment was performed in triplicates, and the percentage of viability was calculated using the following formula:

$$\%\ \text{viability} = \frac{\text{mean OD of BNPs}}{\text{mean OD of control}} \times 100$$

Microscopic Analysis of Promastigotes. To observe promastigote morphology in the presence or absence of Au−Ag BNPs after 48 h, Giemsa (Himedia, India) staining[25] and SEM[25,26] were performed. The images were captured using a light microscope at 100× magnification and an XL30 ESEM-make FEI.

DNA Fragmentation Assay. The genomic DNA of untreated promastigotes and those treated with Au−Ag BNPs for 48 h were extracted using a standard protocol.[27] The fragmentation pattern of genomic DNA was visualized under UV light, and the image was captured using Gel doc 2000 (Bio-Rad).

Estimation of ROS Levels in Promastigotes. To estimate the ROS levels generated inside the promastigotes cultured in the presence or absence of Au−Ag BNPs for 48 h, we used 2′,7′-dichloro dihydrofluorescein diacetate (H_2DCFDA) dye. The ROS levels were measured as MFI by a flow cytometer, BD™ fluorescence-activated cell sorting (FACS) Calibur.[27,28]

Macrophage Culture and Activation. The human monocytic leukemia suspension cell line (THP-1) was obtained from the National Center for Cell Science (Pune, India) and cultured in an RPMI-1640 medium supplemented with 10% (v/v) FBS, glucose 4.5 g/L, 10 mM HEPES, 1 mM sodium pyruvate, 100 U/mL penicillin, and 100 mg/mL streptomycin at 37 °C and 5% CO_2. At the time of experiment, suspension cells were stimulated with 10 ng/mL phorbol 12-myristate 13-acetate (PMA) for 24 h to transform them into macrophage-like phenotypes, which formed a uniform layer on the bottom of the culture plate.

Cytotoxicity Assay on Macrophages. As mentioned above, cytotoxicity of Au−Ag BNPs (concentrations of 0.01, 0.02, 0.04, 0.08, 0.16, 0.32, 0.64, 1.25, and 2.5 μg/mL) was measured against PMA-activated THP-1 macrophages (2×10^4 cells/well) using MTT after 48 h of treatment. Miltefosine (2.5 μM or 1 μg/mL) treatment was the positive control.[27] The experiment was performed in triplicates, and the percentage of macrophage viability was plotted against the BNP concentration.

Microscopic Analysis of the Infection Rate. We performed infectivity studies in 8-well chamber slides by coculturing PMA-activated THP-1 macrophages (2×10^4 cells/well) with early stationary-phase promastigotes in a 1:10 ratio for 6 h. The noninternalized parasites were washed out with sterile 1× PBS (phosphate-buffered saline), and the infected cells were treated with Au−Ag BNPs (0.03−0.035 μg/

https://dx.doi.org/10.1021/acsomega.0c02032
ACS Omega 2020, 5, 16238−16245

mL) for 48 h. Miltefosine (1 μg/mL) was used as the positive control.[27] Slides were developed with Giemsa stain and observed under a light microscope. The experiment was performed three times and each time run in triplicates, and the average number of intracellular amastigotes per 100 macrophages was enumerated.

Measurement of ROS Production Inside Macrophages. According to our previous report,[29] we measured intracellular ROS levels produced in PMA-activated and *L. donovani*-infected macrophages (3×10^4 cells/well) that were cultured in the presence or absence of Au−Ag BNPs for 6 h. We used infected cells without BNP treatment as controls and miltefosine (2.5 μM or 1 μg/mL)-treated cells as positive drug controls for ROS (represented as MFI) levels.

Statistical Analysis. All of the experiments were done in triplicates, and the significance was calculated using the two-tailed unpaired *t*-test (Prism GraphPad software). The *p* values were labeled as $*p \leq 0.05$, $**p \leq 0.01$, and $***p \leq 0.001$.

■ ASSOCIATED CONTENT

Supporting Information

The Supporting Information is available free of charge at https://pubs.acs.org/doi/10.1021/acsomega.0c02032.

Cytotoxicity of Au−Ag BNPs on macrophages (PDF)

■ AUTHOR INFORMATION

Corresponding Authors

Suresh K. Kalangi − *Amity Stem Cell Institute, Amity Medical School, Amity University Haryana, Gurugram, HR 122413, India;* orcid.org/0000-0002-7328-9322; Email: skkalangi@ggn.amity.edu

Radheshyam Maurya − *Department of Animal Biology, School of Life Sciences, University of Hyderabad, Hyderabad, Telangana 500046, India*; Email: rmusl@uohyd.ernet.in

Authors

Dayakar Alti − *Department of Animal Biology, School of Life Sciences, University of Hyderabad, Hyderabad, Telangana 500046, India*

M. Veeramohan Rao − *Department of Physics, Pondicherry University, Puducherry 605014, India*

D. Narayana Rao − *School of Physics, University of Hyderabad, Hyderabad, Telangana 500046, India;* orcid.org/0000-0001-8050-2577

Complete contact information is available at: https://pubs.acs.org/10.1021/acsomega.0c02032

Author Contributions

D.A. helped with the investigation and wrote the first draft, M.V.R. helped in nanoparticle characterizations and interpretation of results, D.N.R. discussed BNP results and helped with editing, and R.M. and S.K.K. helped with the concept, investigation, scoping of the article, result analysis, and editing the final draft.

Notes

The authors declare no competing financial interest.

■ ACKNOWLEDGMENTS

We greatly acknowledge the DST-PURSE fellowship for financial support and DST-FIST for flow cytometry facility, Department of Animal Sciences, University of Hyderabad. R.M. lab acknowledges University of Hyderabad for lab maintenance grant. We thank Suresh Yenugu, Department of Animal Biology, University of Hyderabad, for his critical evaluation and suggestions on writing the manuscript.

■ REFERENCES

(1) Pearson, R. D.; de Queiroz Sousa, A. Clinical spectrum of leishmaniasis. *Clin. Infect. Dis.* **1996**, *22*, 1−11.

(2) WHO Leishmaniasis. March 18, 2018.

(3) Alvar, J.; Aparicio, P.; Aseffa, A.; et al. The relationship between leishmaniasis and AIDS: the second 10 years. *Clin. Microbiol. Rev.* **2008**, *21*, 334−359.

(4) Sacks, D.; Kamhawi, S. Molecular aspects of parasite-vector and vector-host interactions in leishmaniasis. *Annu. Rev. Microbiol.* **2001**, *55*, 453−483.

(5) Sundar, S.; Thakur, B.; Tandon, A.; et al. Clinicoepidemiological study of drug resistance in Indian kala-azar. *BMJ* **1994**, *308*, No. 307.

(6) Mohapatra, S. Drug resistance in leishmaniasis: Newer developments. *Trop. Parasitol.* **2014**, *4*, 4−9.

(7) Laffitte, M. N.; Leprohon, P.; Papadopoulou, B.; Ouellette, M. Plasticity of the Leishmania genome leading to gene copy number variations and drug resistance. *F1000Res.* **2016**, *5*, No. 2350.

(8) Hendrickx, S.; Beyers, J.; Mondelaers, A.; et al. Evidence of a drug-specific impact of experimentally selected paromomycin and miltefosine resistance on parasite fitness in *Leishmania infantum*. *J. Antimicrob. Chemother.* **2016**, *71*, 1914−1921.

(9) Jebali, A.; Kazemi, B. Nano-based antileishmanial agents: a toxicological study on nanoparticles for future treatment of cutaneous leishmaniasis. *Toxicol. In Vitro* **2013**, *27*, 1896−1904.

(10) Ameneh, S.; Khadije, M.; Ahmad-Reza, T.; Omid, R. In *Inhibition of Leishmania Major Growth by Ultraviolet Radiation B with Silver Nanoparticles in an Animal Model*, Paper presented at: Proceedings of the World Congress on Advances in Nano, Biomechanics, Robotics and Energy Research; Seoul, Korea, 2013.

(11) Allahverdiyev, A. M.; Abamor, E. S.; Bagirova, M.; et al. Antileishmanial effect of silver nanoparticles and their enhanced antiparasitic activity under ultraviolet light. *Int. J. Nanomed.* **2011**, *6*, 2705−2714.

(12) Halder, A.; Das, S.; Bera, T.; Mukherjee, A. Rapid synthesis for monodispersed gold nanoparticles in kaempferol and anti-leishmanial efficacy against wild and drug resistant strains. *RSC Adv.* **2017**, *7*, 14159−14167.

(13) Rossi-Bergmann, B.; Pacienza-Lima, W.; Marcato, P. D.; De Conti, R.; Durán, N. Therapeutic potential of biogenic silver nanoparticles in murine cutaneous leishmaniasis. *J. Nano Res.* **2012**, *20*, 89−97.

(14) Begum, N. A.; Mondal, S.; Basu, S.; Laskar, R. A.; Mandal, D. Biogenic synthesis of Au and Ag nanoparticles using aqueous solutions of Black Tea leaf extracts. *Colloids Surf., B* **2009**, *71*, 113−118.

(15) Narayanan, K. B.; Sakthivel, N. Coriander leaf mediated biosynthesis of gold nanoparticles. *Mater. Lett.* **2008**, *62*, 4588−4590.

(16) Philip, D. Spectroscopy B. Biosynthesis of Au, Ag and Au−Ag nanoparticles using edible mushroom extract. *Spectrochim. Acta, Part A* **2009**, *73*, 374−381.

(17) Shankar, S. S.; Rai, A.; Ahmad, A.; Sastry, M. Rapid synthesis of Au, Ag, and bimetallic Au core−Ag shell nanoparticles using Neem (Azadirachta indica) leaf broth. *J. Colloid Interface Sci.* **2004**, *275*, 496−502.

(18) Salunke, G. R.; Ghosh, S.; Kumar, R. S.; et al. Rapid efficient synthesis and characterization of silver, gold, and bimetallic nanoparticles from the medicinal plant Plumbago zeylanica and their application in biofilm control. *Int. J. Nanomed.* **2014**, *9*, 2635−2653.

(19) Ghosh, S.; Jagtap, S.; More, P.; et al. Dioscorea bulbifera mediated synthesis of novel AucoreAgshell nanoparticles with potent antibiofilm and antileishmanial activity. *J. Nanomater.* **2015**, *2015*, No. 562938.

(20) Banerjee, M.; Sharma, S.; Chattopadhyay, A.; Ghosh, S. S. Enhanced antibacterial activity of bimetallic gold-silver core−shell nanoparticles at low silver concentration. *Nanoscale* **2011**, *3*, 5120−5125.
(21) Gopinath, K.; Kumaraguru, S.; Bhakyaraj, K.; et al. Green synthesis of silver, gold and silver/gold bimetallic nanoparticles using the *Gloriosa superba* leaf extract and their antibacterial and antibiofilm activities. *Microb. Pathog.* **2016**, *101*, 1−11.
(22) MubarakAli, D.; Thajuddin, N.; Jeganathan, K.; Gunasekaran, M. Plant extract mediated synthesis of silver and gold nanoparticles and its antibacterial activity against clinically isolated pathogens. *Colloids Surf., B* **2011**, *85*, 360−365.
(23) Allahverdiyev, A. M.; Abamor, E. S.; Bagirova, M.; et al. Investigation of antileishmanial activities of Tio2@ Ag nanoparticles on biological properties of *L. tropica* and *L. infantum* parasites, in vitro. *Exp. Parasitol.* **2013**, *135*, 55−63.
(24) Singh, R.; Nawale, L.; Arkile, M.; et al. Phytogenic silver, gold, and bimetallic nanoparticles as novel antitubercular agents. *Int. J. Nanomed.* **2016**, *11*, 1889−1897.
(25) Dayakar, A.; Chandrasekaran, S.; kumar Prajapati, V.; Veronica, J.; Sundar, S.; Maurya, R. A rapid method to assess the stage differentiation in Leishmania donovani by flow cytometry. *Exp. Parasitol.* **2012**, *132*, 495−500.
(26) Li, Q.; Zhou, Y.; Yao, C.; et al. Apoptosis caused by Hsp90 inhibitor geldanamycin in *Leishmania donovani* during promastigote-to-amastigote transformation stage. *Parasitol. Res.* **2009**, *105*, 1539−1548.
(27) Dayakar, A.; Chandrasekaran, S.; Veronica, J.; Sundar, S.; Maurya, R. In vitro and in vivo evaluation of anti-leishmanial and immunomodulatory activity of Neem leaf extract in *Leishmania donovani* infection. *Exp. Parasitol.* **2015**, *153*, 45−54.
(28) Chandrasekaran, S.; Dayakar, A.; Veronica, J.; Sundar, S.; Maurya, R. An in vitro study of apoptotic like death in *Leishmania donovani* promastigotes by withanolides. *Parasitology international.* **2013**, *62*, 253−261.
(29) Dayakar, A.; Chandrasekaran, S.; Veronica, J.; Maurya, R. Leptin induces the phagocytosis and protective immune response in *Leishmania donovani* infected THP-1 cell line and human PBMCs. *Exp. Parasitol.* **2016**, *160*, 54−59.
(30) Gueirard, P.; Laplante, A.; Rondeau, C.; Milon, G.; Desjardins, M. Trafficking of *Leishmania donovani* promastigotes in non-lytic compartments in neutrophils enables the subsequent transfer of parasites to macrophages. *Cell. Microbiol.* **2008**, *10*, 100−111.
(31) Laufs, H.; Müller, K.; Fleischer, J.; et al. Intracellular survival of *Leishmania major* in neutrophil granulocytes after uptake in the absence of heat-labile serum factors. *Infect. Immun.* **2002**, *70*, 826−835.
(32) Ponte-Sucre, A. Physiological consequences of drug resistance in Leishmania and their relevance for chemotherapy. *Kinetoplastid Biol. Dis.* **2003**, *2*, 14.
(33) Blackwell, J. M. Genetic susceptibility to leishmanial infections: studies in mice and man. *Parasitology* **1996**, *112*, S67−S74.
(34) Chappuis, F.; Sundar, S.; Hailu, A.; et al. Visceral leishmaniasis: what are the needs for diagnosis, treatment and control? *Nat. Rev. Microbiol.* **2007**, *5*, 873−882.
(35) Malafaia, G. Protein-energy malnutrition as a risk factor for visceral leishmaniasis: a review. *Parasite Immunol.* **2009**, *31*, 587−596.
(36) Ponte-Sucre, A.; Gamarro, F.; Dujardin, J.-C.; et al. Drug resistance and treatment failure in leishmaniasis: A 21st century challenge. *PLoS Neglected Trop. Dis.* **2017**, *11*, No. e0006052.
(37) Abamor, E. S.; Allahverdiyev, A. M.; Bagirova, M.; Rafailovich, M. Meglumine antımoniate-TiO2@ Ag nanoparticle combinations reduce toxicity of the drug while enhancing its antileishmanial effect. *Acta Trop.* **2017**, *169*, 30−42.
(38) Soflaei, S.; Dalimi, A.; Ghaffarifar, F.; Shakibaie, M.; Shahverdi, A. R.; Shafiepour, M. In vitro antiparasitic and apoptotic effects of antimony sulfide nanoparticles on Leishmania infantum. *J. Parasitol. Res.* **2012**, *2012*, No. 756568.
(39) Roy, P.; Das, S.; Bera, T.; Mondol, S.; Mukherjee, A. Andrographolide nanoparticles in leishmaniasis: characterization and in vitro evaluations. *eInt. J. Nanomed.* **2010**, *5*, 1113−1121.
(40) Tiwari, B.; Pahuja, R.; Kumar, P.; et al. Nanotized curcumin and miltefosine, a potential combination for treatment of experimental visceral leishmaniasis. *Antimicrob. Agents Chemother.* **2017**, *61*, No. e01169.
(41) Petla, R. K.; Vivekanandhan, S.; Misra, M.; Mohanty, A. K.; Satyanarayana, N. Soybean (Glycine Max) Leaf Extract Based Green Synthesis of Palladium Nanoparticles. *J. Biomater. Nanobiotechnol.* **2012**, *3*, 14−19.
(42) Kruszewski, M.; Brzoska, K.; Brunborg, G.; et al. Toxicity of silver nanomaterials in higher eukaryotes. *Adv. Mol. Toxicol.* **2011**, *5*, 179−218.
(43) Iravani, S. Green synthesis of metal nanoparticles using plants. *Green Chem.* **2011**, *13*, 2638−2650.
(44) Sheny, D.; Mathew, J.; Philip, D. Phytosynthesis of Au, Ag and Au−Ag bimetallic nanoparticles using aqueous extract and dried leaf of Anacardium occidentale. *Spectrochim. Acta, Part A* **2011**, *79*, 254−262.
(45) Mondal, S.; Roy, N.; Laskar, R. A.; et al. Biogenic synthesis of Ag, Au and bimetallic Au/Ag alloy nanoparticles using aqueous extract of mahogany (Swietenia mahogani JACQ.) leaves. *Colloids Surf., B* **2011**, *82*, 497−504.
(46) Jacob, J.; Mukherjee, T.; Kapoor, S. A simple approach for facile synthesis of Ag, anisotropic Au and bimetallic (Ag/Au) nanoparticles using cruciferous vegetable extracts. *Mater. Sci. Eng., C* **2012**, *32*, 1827−1834.
(47) Ahmad, A.; Syed, F.; Shah, A.; et al. Silver and gold nanoparticles from Sargentodoxa cuneata: synthesis, characterization and antileishmanial activity. *RSC Adv.* **2015**, *5*, 73793−73806.
(48) Ghosh, S.; Jagtap, S.; More, P.; et al. Dioscorea bulbifera mediated synthesis of novel Au core Ag shell nanoparticles with potent antibiofilm and antileishmanial activity. *J. Nanomater.* **2015**, *16*, No. 562938.
(49) Dwivedi, A. D.; Gopal, K. Biosynthesis of silver and gold nanoparticles using Chenopodium album leaf extract. *Colloids Surf., A* **2010**, *369*, 27−33.
(50) Mittal, A. K.; Chisti, Y.; Banerjee, U. C. Synthesis of metallic nanoparticles using plant extracts. *Biotechnol. Adv.* **2013**, *31*, 346−356.
(51) Singh, R.; Shedbalkar, U. U.; Wadhwani, S. A.; Chopade, B. A. Bacteriagenic silver nanoparticles: synthesis, mechanism, and applications. *Appl. Microbiol. Biotechnol.* **2015**, *99*, 4579−4593.
(52) Kalangi, S. K.; Dayakar, A.; Gangappa, D.; Sathyavathi, R.; Maurya, R.; Rao, D. N. Biocompatible silver nanoparticles reduced from Anethum graveolens leaf extract augments the antileishmanial efficacy of miltefosine. *Appl. Microbiol. Biotechnol.* **2016**, *170*, 184−192.
(53) Huynh, K. K.; Grinstein, S. Regulation of vacuolar pH and its modulation by some microbial species. *Microbiol. Mol. Biol. Rev.* **2007**, *71*, 452−462.
(54) Jankowski, A.; Scott, C. C.; Grinstein, S. Determinants of the phagosomal pH in neutrophils. *J. Biol. Chem.* **2002**, *277*, 6059−6066.
(55) Xiu, Z-m.; Zhang, Q-b.; Puppala, H. L.; Colvin, V. L.; Alvarez, P. J. J. Negligible particle-specific antibacterial activity of silver nanoparticles. *Nano Lett.* **2012**, *12*, 4271−4275.
(56) Mehta, A.; Shaha, C. Mechanism of metalloid-induced death in Leishmania spp.: role of iron, reactive oxygen species, Ca2+, and glutathione. *Free Radical Biol. Med.* **2006**, *40*, 1857−1868.
(57) Lodge, R.; Descoteaux, A. Phagocytosis of Leishmania donovani amastigotes is Rac1 dependent and occurs in the absence of NADPH oxidase activation. *Eur. J. Immunol.* **2006**, *36*, 2735−2744.
(58) Nwaka, S.; Hudson, A. Innovative lead discovery strategies for tropical diseases. *Nat. Rev. Drug Discovery* **2006**, *5*, 941−955.

https://dx.doi.org/10.1021/acsomega.0c02032
ACS Omega 2020, 5, 16238−16245